Vibration and buckling analysis of functionally graded sandwich beams by a new higher-order shear deformation theory

Trung-Kien Nguyen[a,*], T. Truong-Phong Nguyen[a], Thuc P. Vo[b,**], Huu-Tai Thai[c]

[a] *Faculty of Civil Engineering and Applied Mechanics, University of Technical Education Ho Chi Minh City, 1 Vo Van Ngan Street, Thu Duc District, Ho Chi Minh City, Vietnam*
[b] *Faculty of Engineering and Environment, Northumbria University, Newcastle upon Tyne, NE1 8ST, UK.*
[c] *Centre for Infrastructure Engineering and Safety, School of Civil and Environmental Engineering, The University of New South Wales, Sydney, NSW 2052, Australia*

Abstract

This paper proposes a new higher-order shear deformation theory for buckling and free vibration analysis of isotropic and functionally graded (FG) sandwich beams. The present theory accounts a new hyperbolic distribution of transverse shear stress and satisfies the traction free boundary conditions. Equations of motion are derived from Lagrange's equations. Analytical solutions are presented for the isotropic and FG sandwich beams with various boundary conditions. Numerical results for natural frequencies and critical buckling loads obtained using the present theory are compared with those obtained using the higher and first-order shear deformation beam theories. Effects of the boundary conditions, power-law index, span-to-depth ratio and skin-core-skin thickness ratios on the critical buckling loads and natural frequencies of the FG beams are discussed.

Keywords: A. Hybrid; C. Numerical analysis

1. Introduction

Functionally graded materials (FGMs) are composite materials formed of two or more constituent phases with a continuously variable composition. Sandwich structures are widely employed in aerospace and many other industries. These structures become even more attractive due to the introduction of FGMs for the faces and the core. Typically, there are three typical FG beams: isotropic FG beams, sandwich beams with homogeneous core and FG faces, and sandwich beams with FG core and homogeneous faces.

It is known that the behaviours of isotropic and FG sandwich beams can be predicted by classical beam theory (CBT) ([1–5]), first-order shear deformation beam theory (FSBT) ([6–12]) and higher-

*Corresponding author, tel.: +848 3897 2092
**Corresponding author, tel.: +44 191 243 7856
Email addresses: kiennt@hcmute.edu.vn (Trung-Kien Nguyen), thuc.vo@northumbria.ac.uk (Thuc P. Vo)

order shear deformation beam theory (HSBT) ([1, 13–31]) or three-dimensional (3D) elasticity theory ([32–34]). It should be noted that Carrera et al. ([23],[24]) developed Carrera Unified Formulation (CUF) which can generate any refined theories for beams, plates and shells. This formulation was used extensively for various structural problems and only a few of them are cited here, for instance, static and vibration analysis of FG beams ([25]-[27]) and FG plates and shells ([28]-[31]). It is well-known that the CBT is applicable to slender beams only. For moderate beams, it underestimates deflection and overestimates buckling load and natural frequencies due to ignoring the shear deformation effect. In order to include this effect, a shear correction factor is required for FSBT but not for HSBT. However, the efficiency of the HSBT depends on the appropriate choice of displacement field which is an interesting subject attracted many researchers ([1, 14, 19, 22, 35–41]).

The objective of this paper is to present a new higher-order shear deformation theory for buckling and vibration analysis of isotropic and FG sandwich beams. Equations of motion are derived from Lagrange's equations. The FG beam is assumed to have isotropic, two-constituent material distribution through the depth, and Young's modulus is assumed to vary according to power-law form. Analytical solutions are derived for various boundary conditions to investigate the effects of the boundary conditions, power-law index, span-to-depth ratio and skin-core-skin thickness ratios on the critical buckling loads and natural frequencies of the FG beams.

2. Theoretical formulation

2.1. FG sandwich beams

Consider a beam as shown in Fig. 1 with length L and uniform section $b \times h$. The beam is made of a mixture of ceramic and metal isotropic materials whose properties vary smoothly through the depth according to the volume fractions of the constituents. Three different types of the FG beams are considered: isotropic FG beams (type A), sandwich beams with FG faces and homogeneous core (type B), and sandwich beams with FG core and homogeneous faces (type C).

2.1.1. Type A: isotropic FG beams

The beam of type A is graded from metal located at the bottom surface to ceramic material at the top surface (Fig. 1b). The volume fraction of ceramic material V_c is given as follows:

$$V_c(z) = \left(\frac{2z+h}{2h}\right)^p \tag{1}$$

.

where p is the scalar parameter, which is positive and $z \in [-\frac{h}{2}, \frac{h}{2}]$.

2.1.2. Type B: sandwich beams with FG faces and homogeneous core

The faces of this type are graded from metal to ceramic and the core is made of isotropic ceramic (Fig. 1c). The volume fraction function of ceramic phase $V_c^{(j)}$ given by:

$$\begin{cases} V_c^{(1)}(z) = \left(\frac{z-h_0}{h_1-h_0}\right)^p & \text{for} \quad z \in [h_0, h_1] \\ V_c^{(2)}(z) = 1 & \text{for} \quad z \in [h_1, h_2] \\ V_c^{(3)}(z) = \left(\frac{z-h_3}{h_2-h_3}\right)^p & \text{for} \quad z \in [h_2, h_3] \end{cases} \tag{2}$$

2.1.3. Type C: sandwich beams with FG core and homogeneous faces

The core layer of this type is graded from metal to ceramic. The lower face is made of isotropic metal, whereas the upper face is isotropic ceramic (Fig. 1d). The volume fraction function of ceramic material of the j-th layer $V_c^{(j)}$ defined by:

$$\begin{cases} V_c^{(1)}(z) = 0 & \text{for} \quad z \in [h_0, h_1] \\ V_c^{(2)}(z) = \left(\frac{z-h_1}{h_2-h_1}\right)^p & \text{for} \quad z \in [h_1, h_2] \\ V_c^{(3)}(z) = 1 & \text{for} \quad z \in [h_2, h_3] \end{cases} \tag{3}$$

The variation of V_c through the beam depth for three types is displayed in Fig. 2. The material property distribution of FG beam through its depth is given by the power-law form:

$$P(z) = (P_c - P_m)V_c(z) + P_c \tag{4}$$

where P_c and P_m are Young's modulus (E), Poisson's ratio (ν), mass density (ρ) of ceramic and metal materials, respectively.

2.2. Higher-order shear deformation beam theory

The displacement field of the present theory is given by:

$$U(x,z) = u(x) - zw_{,x} + f(z)\theta(x) \tag{5a}$$

$$W(x,z) = w(x) \tag{5b}$$

where

$$f(z) = \cot^{-1}\left(\frac{h}{z}\right) - \frac{16z^3}{15h^3} \tag{6}$$

and u, θ are the mid-plane axial displacement and rotation, w denotes the mid-plane transverse displacement of the beam, the comma indicates partial differentiation with respect to the coordinate subscript that follows.

The nonzero strains associated with the displacement field in Eq. (5) are:

$$\epsilon_{xx}(x,z) = \epsilon^0_{xx} + z\kappa^b_{xx} + f\kappa^s_{xx} \tag{7a}$$

$$\gamma_{xz}(x,z) = g(z)\theta \tag{7b}$$

where $g(z) = f_{,z}$; ϵ^0_{xx} and κ^b_{xx}, κ^s_{xx} are the axial strain and curvatures of the beam, respectively. These components are related with the displacements u, w and θ of the beam as follows:

$$\epsilon^0_{xx}(x) = u_{,x}, \quad \kappa^b_{xx}(x) = -w_{,xx}, \quad \kappa^s_{xx}(x) = \theta_{,x} \tag{8}$$

The strains and stresses are related by:

$$\sigma_{xx}(x,z) = E(z)\left[\epsilon^0_{xx}(x) + z\kappa^b_{xx}(x) + f\kappa^s_{xx}(x)\right] \tag{9a}$$

$$\sigma_{xz}(x,z) = G(z)\gamma_{xz}(x,z) \tag{9b}$$

where $G(z) = E(z)/2(1+\nu(z))$ is shear modulus at location z.

2.3. Variational formulation

In order to derive the equations of motion, Lagrangian functional is used:

$$\Pi = \mathcal{U} + \mathcal{V} - \mathcal{K} \tag{10}$$

where $\mathcal{U}$, $\mathcal{V}$ and $\mathcal{K}$ denote the strain energy, work done, and kinetic energy, respectively.

The strain energy of the beam is calculated by:

$$\begin{aligned}\mathcal{U} &= \frac{1}{2}\int_V (\sigma_{xx}\epsilon_{xx} + \sigma_{xz}\gamma_{xz})dV \\ &= \frac{1}{2}\int_0^L \Big[A(u_{,x})^2 - 2Bu_{,x}w_{,xx} + D(w_{,xx})^2 + 2B^s u_{,x}\theta_{,x} - 2D^s w_{,xx}\theta_{,x} \\ &+ H^s(\theta_{,x})^2 + A^s\theta^2\Big]dx\end{aligned} \tag{11}$$

where (A, B, D, B^s, D^s, H^s) are the stiffnesses of FG beams given by:

$$(A, B, D, B^s, D^s, H^s) = \int_{-h/2}^{h/2} (1, z, z^2, f, zf, f^2)E(z)bdz \tag{12}$$

$$A^s = \int_{-h/2}^{h/2} g^2 G(z) b dz \tag{13}$$

The work done by the axial compressive load N_0 can be expressed as:

$$\mathcal{V} = \frac{1}{2}\int_0^L N_0 (w_{,x})^2 dx \tag{14}$$

The kinetic energy is obtained as:

$$\begin{aligned}\mathcal{K} &= \frac{1}{2}\int_V \rho(z)(\dot{U}^2 + \dot{W}^2) dV \\ &= \frac{1}{2}\int_0^L \Big[I_0 \dot{u}^2 - 2I_1 \dot{u}\dot{w}_{,x} + I_2 (\dot{w}_{,x})^2 + 2J_1 \dot{\theta}\dot{u} - 2J_2 \dot{\theta}\dot{w}_{,x} + K_2 \dot{\theta}^2 + I_0 \dot{w}^2 \Big] dx \end{aligned} \tag{15}$$

where the differentiation with respect to the time t is denoted by dot-superscript convention; ρ is the mass density of each layer and $I_0, I_1, I_2, J_1, J_2, K_2$ are the inertia coefficients defined by:

$$(I_0, I_1, I_2, J_1, J_2, K_2) = \int_{-h/2}^{h/2} \rho(z)(1, z, z^2, f, zf, f^2) b dz \tag{16}$$

By substituting Eqs. (11), (14) and (15) into Eq. (10), Lagrangian functional is explicitly expressed as:

$$\begin{aligned}\Pi = &\frac{1}{2}\int_0^L \Big[A(u_{,x})^2 - 2Bu_{,x}w_{,xx} + D(w_{,xx})^2 + 2B^s u_{,x}\theta_{,x} - 2D^s w_{,xx}\theta_{,x} + H^s(\theta_{,x})^2 + A^s\theta^2 \Big] dx \\ &+ \frac{1}{2}\int_0^L N_0 (w_{,x})^2 dx - \frac{1}{2}\int_0^L \Big[I_0 \dot{u}^2 - 2I_1 \dot{u}\dot{w}_{,x} + I_2 (\dot{w}_{,x})^2 + 2J_1 \dot{\theta}\dot{u} - 2J_2 \dot{\theta}\dot{w}_{,x} + K_2 \dot{\theta}^2 + I_0 \dot{w}^2 \Big] dx \end{aligned} \tag{17}$$

In order to derive the equations of motion, the displacement field is approximated as the following forms:

$$u(x,t) = \sum_{j=1}^{m} \psi_j(x) u_j e^{i\omega t} \tag{18a}$$

$$w(x,t) = \sum_{j=1}^{m} \varphi_j(x) w_j e^{i\omega t} \tag{18b}$$

$$\theta(x,t) = \sum_{j=1}^{m} \psi_j(x) \theta_j e^{i\omega t} \tag{18c}$$

where ω is the frequency of free vibration of the beam, $\sqrt{i} = -1$ the imaginary unit, (u_j, w_j, θ_j) denotes the values to be determined, $\psi_j(x)$ and $\varphi_j(x)$ are the shape functions. By substituting Eq. (18) into Eq. (17), and using Lagrange's equations:

$$\frac{\partial \Pi}{\partial q_j} - \frac{d}{dt}\frac{\partial \Pi}{\partial \dot{q}_j} = 0 \tag{19}$$

with q_j representing the values of (u_j, w_j, θ_j), that leads to:

$$\left(\begin{bmatrix} \mathbf{K}^{11} & \mathbf{K}^{12} & \mathbf{K}^{13} \\ {}^T\mathbf{K}^{12} & \mathbf{K}^{22} & \mathbf{K}^{23} \\ {}^T\mathbf{K}^{13} & {}^T\mathbf{K}^{23} & \mathbf{K}^{33} \end{bmatrix} - \omega^2 \begin{bmatrix} \mathbf{M}^{11} & \mathbf{M}^{12} & \mathbf{M}^{13} \\ {}^T\mathbf{M}^{12} & \mathbf{M}^{22} & \mathbf{M}^{23} \\ {}^T\mathbf{M}^{13} & {}^T\mathbf{M}^{23} & \mathbf{M}^{33} \end{bmatrix} \right) \begin{Bmatrix} \mathbf{u} \\ \mathbf{w} \\ \boldsymbol{\theta} \end{Bmatrix} = \begin{Bmatrix} \mathbf{0} \\ \mathbf{0} \\ \mathbf{0} \end{Bmatrix} \tag{20}$$

where the components of the stiffness matrix $\mathbf{K}$ and the mass matrix $\mathbf{M}$ are given as follows:

$$\begin{aligned}
K_{ij}^{11} &= A\int_0^L \psi_{i,x}\psi_{j,x}\,dx, K_{ij}^{12} = -B\int_0^L \psi_{i,x}\varphi_{j,xx}\,dx, K_{ij}^{13} = B^s\int_0^L \psi_{i,x}\psi_{j,x}\,dx \\
K_{ij}^{22} &= D\int_0^L \varphi_{i,xx}\varphi_{j,xx}\,dx - N^0\int_0^L \varphi_{i,x}\varphi_{j,x}\,dx, K_{ij}^{23} = -D^s\int_0^L \varphi_{i,xx}\psi_{j,x}\,dx \\
K_{ij}^{33} &= H^s\int_0^L \psi_{i,x}\psi_{j,x}\,dx + A^s\int_0^L \psi_i\psi_j\,dx \\
M_{ij}^{11} &= I_0\int_0^L \psi_i\psi_j\,dx, M_{ij}^{12} = -I_1\int_0^L \psi_i\varphi_{j,x}\,dx, M_{ij}^{13} = J_1\int_0^L \psi_i\psi_j\,dx \\
M_{ij}^{22} &= I_0\int_0^L \varphi_i\varphi_j\,dx + I_2\int_0^L \varphi_{i,x}\varphi_{j,x}\,dx, M_{ij}^{23} = -J_2\int_0^L \varphi_{i,x}\psi_j\,dx \\
M_{ij}^{33} &= K_2\int_0^L \psi_i\psi_j\,dx
\end{aligned} \tag{21}$$

The solution of Eq. (20) will allow to calculate the critical buckling loads (N_{cr}) and natural frequencies of isotropic and FG sandwich beams.

2.4. Analytical solutions

To derive analytical solutions, the shape functions $\psi(x)$ and $\varphi(x)$ are chosen for various boundary conditions (S-S: simply supported, C-C: clamped-clamped, and C-F: clamped-free beams) as follows:

$$\psi(x) = x^{j-1},\ \varphi(x) = x^{j-1} \tag{22}$$

In order to impose the various boundary conditions, the method of Lagrange multipliers can be used so that the Lagrangian functional of the problem is rewritten as follows:

$$\Pi^* = \Pi + \beta_i\hat{u}_i(\bar{x}) \tag{23}$$

where β_i are the Lagrange multipliers which are the support reactions of the problem, $\hat{u}_i(\bar{x})$ denote the values of prescribed displacement at location $\bar{x} = 0, L$. By using Lagrange's equations (Eq. (19)), a new characteristic problem for buckling and free vibration analysis is obtained as follows:

$$\left(\begin{bmatrix} \mathbf{K}^{11} & \mathbf{K}^{12} & \mathbf{K}^{13} & \mathbf{K}^{14} \\ {}^T\mathbf{K}^{12} & \mathbf{K}^{22} & \mathbf{K}^{23} & \mathbf{K}^{24} \\ {}^T\mathbf{K}^{13} & {}^T\mathbf{K}^{23} & \mathbf{K}^{33} & \mathbf{K}^{34} \\ {}^T\mathbf{K}^{14} & {}^T\mathbf{K}^{24} & {}^T\mathbf{K}^{34} & \mathbf{0} \end{bmatrix} - \omega^2 \begin{bmatrix} \mathbf{M}^{11} & \mathbf{M}^{12} & \mathbf{M}^{13} & \mathbf{0} \\ {}^T\mathbf{M}^{12} & \mathbf{M}^{22} & \mathbf{M}^{23} & \mathbf{0} \\ {}^T\mathbf{M}^{13} & {}^T\mathbf{M}^{23} & \mathbf{M}^{33} & \mathbf{0} \\ \mathbf{0} & \mathbf{0} & \mathbf{0} & \mathbf{0} \end{bmatrix}\right) \begin{Bmatrix} \mathbf{u} \\ \mathbf{w} \\ \boldsymbol{\theta} \\ \boldsymbol{\beta} \end{Bmatrix} = \begin{Bmatrix} \mathbf{0} \\ \mathbf{0} \\ \mathbf{0} \\ \mathbf{0} \end{Bmatrix} \tag{24}$$

where the components of matrix $\mathbf{K}^{14}$, $\mathbf{K}^{24}$ and $\mathbf{K}^{34}$ depend on number of boundary conditions and associated prescribed displacements (Table 1). For C-C beams, these stiffness components are given

by:

$$K_{i1}^{14} = \psi_i(0),\ K_{i2}^{14} = \psi_i(L),\ K_{ij}^{14} = 0 \quad \text{with} \quad j = 3, 4, ..., 8 \tag{25a}$$

$$K_{i3}^{24} = \varphi_i(0),\ K_{i4}^{24} = \varphi_i(L),\ K_{i5}^{24} = \varphi_{i,x}(0),\ K_{i6}^{24} = \varphi_{i,x}(L), K_{ij}^{24} = 0 \quad \text{with} \quad j = 1, 2, 7, 8 \tag{25b}$$

$$K_{i7}^{34} = \psi_i(0),\ K_{i8}^{34} = \psi_i(L),\ K_{ij}^{34} = 0 \quad \text{with} \quad j = 1, 2, ..., 6 \tag{25c}$$

3. Numerical results and discussion

In this section, a number of numerical examples are analyzed in order to verify the accuracy of present study and investigate the critical buckling loads and natural frequencies of isotropic and FG sandwich beams. Three types of FG beams (types A, B and C) are constituted by a mixture of isotropic ceramic (Al_2O_3) and metal (Al). The material properties of Al_2O_3 are: E_c=380 GPa, ν_c=0.3, ρ_c=3960 kg/m^3, and those of Al are: E_m=70 GPa, ν_m=0.3, ρ_m=2702 kg/m^3. Effects of the power-law index, span-to-depth ratio, skin-core-skin thickness ratios and boundary conditions on the buckling and vibration behaviours of the isotropic and FG sandwich beams are discussed in details. Three boundary conditions (BC) are considered (C-C, S-S and C-F) and these kinetic boundary conditions are given in Table 1. For simplicity, the non-dimensional natural frequencies and critical buckling loads are defined as:

$$\bar{\omega} = \frac{\omega L^2}{h}\sqrt{\frac{\rho_m}{E_m}},\ \bar{N}_{cr} = N_{cr}\frac{12L^2}{E_m h^3} \tag{26}$$

In order to verify the convergence of the present polynomial series solution, Table 2 presents the fundamental frequency and critical buckling loads for three boundary conditions of FG beams (type A). The solutions are calculated for the power-law index (p=1) and span-to-depth ratio (L/h=5). It can be seen that the solutions of S-S and C-F boundary conditions converge more quickly than C-C one. The number of terms m=14 is sufficient to obtain an accurate solution and thus, this number is used throughout the numerical examples.

As the first example, Tables 3-5 present the comparison of the natural frequencies and critical buckling loads of FG beams (type A) with three boundary conditions. They are calculated for various values of the power-law index and compared to the solutions obtained from the FSBT ([9, 10]) and third-order shear deformation beam theory (TSBT) ([17, 21, 22]). It is seen that the solutions obtained derived from the proposed theory are in excellent agreement with those obtained from previous results for both deep and thin beams. Fig. 3 displays the variation of the fundamental frequency and critical buckling load with respect to the power-law index and span-to-depth ratio of FG beams. Three curves are observed for three boundary conditions, the highest curve corresponds to the C-C case and the

lowest one is the C-F case. It can be seen that the results decrease with an increase of the power-law index.

In the following case, the first five natural frequencies of a cantilever sandwich beam, which is made up of two steel (Fe) faces and Aluminum/Zirconia (Al/ZrO_2) core, are calculated. The material properties are: Al ($E_m = 70\text{GPa}, \nu_m = 0.3, \rho_m = 2700\text{kg/m}^3$) and ZrO_2 ($E_c = 151\text{GPa}, \nu_c = 0.3, \rho_c = 5700\text{kg/m}^3$) and Fe ($E_f = 210\text{GPa}, \nu_f = 0.3, \rho_f = 7860\text{kg/m}^3$). The face and core thicknesses are 3 and 14 mm, whereas the length and cross-section are 200 mm and 20 mm×20 mm. The results are given in Table 6 along with those of Mashat et al. [26] using the CUF (TE1^{zz} and E4-4$_2$) and Bui et al. [42] using meshfree method. The natural frequencies computed in present theory agree well with the reference solutions.

In order to validate of the present theory further, the natural frequencies and critical buckling loads of Al/Al_2O_3 sandwich beams of type B are compared with those obtained from TSBT [17] in Tables 7-10. They are carried out for six values of skin-core-skin thickness ratios with different values of the power-law index. It can be seen again that the present theory provides excellent agreement solution for type B beams. It implies that the proposed theory is appropriate and efficient for analyzing vibration and buckling responses of sandwich beams. The lowest and highest values of natural frequency and critical buckling load correspond to the (1-0-1) and (1-2-1) sandwich beams. It is due to the fact that these beams correspond to the lowest and highest volume fractions of the ceramic phase. The effect of the span-to-depth ratio on the buckling and vibration response of symmetric (2-1-2) and non-symmetric (2-1-1) sandwich beams is plotted in Figs. 4 and 5, it can be seen that the effect of the shear deformation is negligible except for the case of the C-C beam where this effect is significant with $L/h \leq 10$.

Finally, the first three natural frequencies and critical buckling loads of (1-2-1) and (2-2-1) Al/Al_2O_3 sandwich beams of type C are given in Tables 11 and 12. Their variations with respect to the span-to-depth ratio L/h are plotted in Figs. 6 and 7. The results clearly indicate that the shear deformation effect is remarkably significant for the case of thick or moderately thick beams, but it is negligible for the case of thin beams ($L/h \geq 25$). Due to higher ceramic portion, the results of (1-2-1) sandwich beam are greater than those of (2-2-1) one. They are the maximum for $p = 0$ and the minimum for $p = 10$. A simply supported sandwich beam is chosen to investigate the vibration mode shapes with the power-law index $p = 10$ in Fig. 8. Due to unsymmetric beam, it can be seen that all three modes display triply coupled vibration.

4. Conclusions

A new higher-order shear deformation theory is presented for buckling and free vibration analysis of isotropic and FG sandwich beams. The proposed theory accounts a new hyperbolic distribution of transverse shear stress and satisfies the traction free boundary conditions. Analytical polynomial series solutions are derived for three types of FG beams with various boundary conditions. Effects of the boundary conditions, power-law index, span-to-depth ratio and skin-core-skin thickness ratios on the critical buckling loads and natural frequencies are discussed. The obtained solutions are in excellent agreement with those derived from earlier works. The proposed theory is accurate and efficient in solving the free vibration and buckling behaviours of the isotropic and FG sandwich beams.

Acknowledgements

This research is funded by University of Technical Education Ho Chi Minh City. The support is gratefully acknowledged.

References

[1] M. Aydogdu, V. Taskin, Free vibration analysis of functionally graded beams with simply supported edges, Materials and Design 28 (2007) 1651–1656.

[2] J. Yang, Y. Chen, Free vibration and buckling analyses of functionally graded beams with edge cracks, Composite Structures 83 (2008) 48–60.

[3] M. Simsek, T. Kocaturk, Free and forced vibration of a functionally graded beam subjected to a concentrated moving harmonic load, Composite Structures 90 (4) (2009) 465 – 473.

[4] S. Pradhan, T. Murmu, Thermo-mechanical vibration of FGM sandwich beam under variable elastic foundations using differential quadrature method, Journal of Sound and Vibration 321 (1-2) (2009) 342 – 362.

[5] H. Su, J. R. Banerjee, C. W. Cheung, Dynamic stiffness formulation and free vibration analysis of functionally graded beams, Composite Structures , 106 (2013) 854 – 862

[6] A. Chakraborty, S. Gopalakrishnan, J. N. Reddy, A new beam finite element for the analysis of functionally graded materials, International Journal of Mechanical Sciences 45 (3) (2003) 519 – 539.

[7] X.-F. Li, A unified approach for analyzing static and dynamic behaviors of functionally graded Timoshenko and Euler-Bernoulli beams, Journal of Sound and Vibration 318 (45) (2008) 1210 – 1229.

[8] S. Sina, H. Navazi, H. Haddadpour, An analytical method for free vibration analysis of functionally graded beams, Materials and Design 30 (3) (2009) 741 – 747.

[9] S.-R. Li, R. C. Batra, Relations between buckling loads of functionally graded Timoshenko and homogeneous Euler-Bernoulli beams, Composite Structures 95 (2013) 5 – 9.

[10] T.-K. Nguyen, T. P. Vo, H.-T. Thai, Static and free vibration of axially loaded functionally graded beams based on the first-order shear deformation theory, Composites Part B: Engineering 55 (2013) 147 – 157.

[11] K. Pradhan, S. Chakraverty, Free vibration of Euler and Timoshenko functionally graded beams by Rayleigh-Ritz method, Composites Part B: Engineering 51 (2013) 175 – 184.

[12] H. Su, J. R. Banerjee, Development of dynamic stiffness method for free vibration of functionally graded Timoshenko beams, Computers & Structures, 147 (2015) 107– 116

[13] S. Kapuria, M. Bhattacharyya, A. N. Kumar, Bending and free vibration response of layered functionally graded beams: A theoretical model and its experimental validation, Composite Structures 82 (3) (2008) 390 – 402.

[14] R. Kadoli, K. Akhtar, N. Ganesan, Static analysis of functionally graded beams using higher order shear deformation theory, Applied Mathematical Modelling 32 (12) (2008) 2509 – 2525.

[15] X.-F. Li, B.-L. Wang, J.-C. Han, A higher-order theory for static and dynamic analyses of functionally graded beams, Archive of Applied Mechanics 80 (2010) 1197–1212.

[16] T. P. Vo, H.-T. Thai, T.-K. Nguyen, F. Inam, Static and vibration analysis of functionally graded beams using refined shear deformation theory, Meccanica 49 (1) (2014) 155–168.

[17] T. P. Vo, H.-T. Thai, T.-K. Nguyen, A. Maheri, J. Lee, Finite element model for vibration and buckling of functionally graded sandwich beams based on a refined shear deformation theory, Engineering Structures 64 (2014) 12 – 22.

[18] M. A. Benatta, I. Mechab, A. Tounsi, E. A. A. Bedia, Static analysis of functionally graded short beams including warping and shear deformation effects, Computational Materials Science 44 (2) (2008) 765 – 773.

[19] S. Ben-Oumrane, T. Abedlouahed, M. Ismail, B. B. Mohamed, M. Mustapha, A. B. E. Abbas, A theoretical analysis of flexional bending of Al/Al2O3 S-FGM thick beams, Computational Materials Science 44 (4) (2009) 1344 – 1350.

[20] A. M. Zenkour, M. N. M. Allam, M. Sobhy, Bending analysis of FG viscoelastic sandwich beams with elastic cores resting on Pasternaks elastic foundations, Acta Mechanica 212 (2010) 233–252.

[21] H. T. Thai, T. P. Vo, Bending and free vibration of functionally graded beams using various higher-order shear deformation beam theories, International Journal of Mechanical Sciences 62 (1) (2012) 57–66.

[22] M. Simsek, Fundamental frequency analysis of functionally graded beams by using different higher-order beam theories, Nuclear Engineering and Design 240 (4) (2010) 697 – 705.

[23] E. Carrera, Theories and finite elements for multilayered plates and shells:a unified compact formulation with numerical assessment and benchmarking, Archives of Computational Methods in Engineering 10 (3) (2003) 215–296.

[24] E. Carrera, G. Giunta, M. Petrolo, Beam structures: classical and advanced theories, John Wiley & Sons, 2011.

[25] G. Giunta, S. Belouettar, E. Carrera, Analysis of FGM Beams by Means of Classical and Advanced Theories, Mechanics of Advanced Materials and Structures 17 (8) (2010) 622–635.

[26] D. S. Mashat, E. Carrera, A. M. Zenkour, S. A. A. Khateeb, M. Filippi, Free vibration of FGM layered beams by various theories and finite elements, Composites Part B: Engineering 59 (2014) 269 – 278.

[27] M. Filippi, E. Carrera, A. M. Zenkour. Static analyses of FGM beams by various theories and finite elements, Composites Part B: Engineering 72 (2015) 1 – 9

[28] E. Carrera, S. Brischetto, M. Cinefra, M. Soave, Effects of thickness stretching in functionally graded plates and shells, Composites Part B: Engineering 42 (2) (2011) 123 – 133.

[29] F. Tornabene, N. Fantuzzi, M. Bacciocchi. Free vibrations of free-form doubly-curved shells made of functionally graded materials using higher-order equivalent single layer theories, Composites Part B: Engineering 67 (2014) 490 – 509

[30] F. Tornabene, N. Fantuzzi, E. Viola, R. C. Batra. Stress and strain recovery for functionally graded free-form and doubly-curved sandwich shells using higher-order equivalent single layer theory, Composite Structures 119 (2015) 67 – 89

[31] N. Fantuzzi, F. Tornabene, E. Viola. Four-Parameter Functionally Graded Cracked Plates of Arbitrary Shape: a GDQFEM Solution for Free Vibrations, Mechanics of Advanced Materials and Structures 2015, In Press.

[32] B. V. Sankar, An elasticity solution for functionally graded beams, Composites Science and Technology 61 (5) (2001) 689 – 696.

[33] Z. Zhong, T. Yu, Analytical solution of a cantilever functionally graded beam, Composites Science and Technology 67 (34) (2007) 481 – 488.

[34] M. Kashtalyan, M. Menshykova, Three-dimensional elasticity solution for sandwich panels with a functionally graded core, Composite Structures 87 (1) (2009) 36 – 43.

[35] J. N. Reddy, A simple higher-order theory for laminated composite plates, Journal of Applied Mechanics 51 (1984) 745–752.

[36] M. Touratier, An efficient standard plate theory, International Journal of Engineering Science 29 (8) (1991) 901 – 916.

[37] K. Soldatos, A transverse shear deformation theory for homogeneous monoclinic plates, Acta Mechanica 94 (3-4) (1992) 195–220.

[38] M. Karama, K. Afaq, S. Mistou, Mechanical behaviour of laminated composite beam by the new multi-layered laminated composite structures model with transverse shear stress continuity, International Journal of Solids and Structures 40 (6) (2003) 1525 – 1546.

[39] X. F. Li, B. L. Wang, J. C. Han, A higher-order theory for static and dynamic analyses of functionally graded beams, Archive of Applied Mechanics 80 (2010) 1197–1212.

[40] N. Wattanasakulpong, B. G. Prusty, D. W. Kelly, Thermal buckling and elastic vibration of third-order shear deformable functionally graded beams, International Journal of Mechanical Sciences 53 (2011) 734–743.

[41] V.-H. Nguyen, T.-K. Nguyen, H.-T. Thai, T. P. Vo, A new inverse trigonometric shear deformation theory for isotropic and functionally graded sandwich plates, Composites Part B: Engineering 66 (2014) 233 – 246.

[42] T. Bui, A. Khosravifard, C. Zhang, M. Hematiyan, M. Golub, Dynamic analysis of sandwich beams with functionally graded core using a truly meshfree radial point interpolation method, Engineering Structures 47 (0) (2013) 90 – 104.

CAPTIONS OF TABLES

Table 1: Kinematic boundary conditions.

Table 2: Convergence of the nondimensional fundamental frequency and critical buckling load of FG beams with $p = 1$ and $L/h = 5$ (type A).

Table 3: Comparison of the first three nondimensional natural frequencies of S-S FG beams (type A).

Table 4: Comparison of the nondimensional fundamental natural frequency of FG beams with various boundary conditions (L/h=5 and 20, type A).

Table 5: Comparison of the nondimensional critical buckling load of FG beams with various boundary conditions (L/h=5 and 10, type A).

Table 6: The first five natural frequencies of a cantilever sandwich beam with a FG core and isotropic faces (p=1).

Table 7: Nondimensional fundamental frequency ($\bar{\omega}$) of FG sandwich beams with various boundary conditions (L/h=5, type B).

Table 8: Nondimensional fundamental frequency ($\bar{\omega}$) of FG sandwich beams with various boundary conditions (L/h=20, type B).

Table 9: Nondimensional critical buckling load ($\bar{N}_{cr}$) of FG sandwich beams with various boundary conditions (L/h=5, type B).

Table 10: Nondimensional critical buckling load ($\bar{N}_{cr}$) of FG sandwich beams with various boundary conditions (L/h=20, type B).

Table 11: The first three nondimensional natural frequencies of FG sandwich beams with various boundary conditions (type C).

Table 12: Nondimensional critical buckling load of FG sandwich beams with various boundary conditions (type C).

CAPTIONS OF FIGURES

Figure 1: Geometry of isotropic and FG sandwich beams.

Figure 2: Distribution of ceramic material through the beam depth according to the power-law form.

Figure 3: Effects of the power-law index p, span-to-depth ratio L/h on the nondimensional fundamental frequency ($\bar{\omega}$) and critical buckling load ($\bar{N}_{cr}$) of FG beams (type A).

Figure 4: Variation of the nondimensional fundamental frequency of FG sandwich beams ($p = 10$) with respect to the span-to-depth ratio L/h (type B).

Figure 5: Variation of the nondimensional critical buckling load of FG sandwich beams ($p = 10$) with respect to the span-to-depth ratio L/h (type B).

Figure 6: Variation of the nondimensional fundamental frequency of (C-C) FG sandwich beams with respect to the span-to-depth ratio L/h (type C).

Figure 7: Variation of the nondimensional critical buckling load of (C-C) FG sandwich beams with respect to the span-to-depth ratio L/h (type C).

Figure 8: The first three mode shapes of (1-2-1) and (2-2-1) (S-S) FG sandwich beams ($L/h = 5$, $p = 10$, type C).

Table 1: Kinematic boundary conditions.

BC	$x = 0$	$x = L$
S-S	$w = 0$	$w = 0$
C-F	$u = 0$, $w = 0$, θ=0, $w_{,x}$=0	
C-C	$u = 0$, $w = 0$, θ=0, $w_{,x}$=0	$u = 0$, $w = 0$, θ=0, $w_{,x}$=0

Table 2: Convergence of the nondimensional fundamental frequency and critical buckling load of FG beams with $p = 1$ and $L/h = 5$ (type A).

BC	Number of terms (m)						
	6	8	10	12	14	16	18
Fundamental frequency							
S-S	3.9907	3.9904	3.9904	3.9904	3.9904	3.9904	3.9904
C-F	1.4645	1.4638	1.4635	1.4633	1.4633	1.4633	1.4633
C-C	8.0309	8.0031	7.9704	7.9572	7.9518	7.9500	7.9493
Critical buckling load							
S-S	24.5873	24.5840	24.5840	24.5840	24.5840	24.5840	24.5840
C-F	6.5352	6.5352	6.5352	6.5352	6.5352	6.5352	6.5352
C-C	81.3950	79.4992	79.4888	79.4888	79.4888	79.4888	79.4888

Table 3: Comparison of the first three nondimensional natural frequencies of S-S FG beams (type A).

L/h	Mode	Theory	p					
			0	0.5	1	2	5	10
5	1	Present	5.1528	4.4102	3.9904	3.6264	3.4009	3.2815
		FSBT [10]	5.1525	4.4075	3.9902	3.6344	3.4312	3.3135
		TSBT [21]	5.1527	4.4107	3.9904	3.6264	3.4012	3.2816
	2	Present	17.8817	15.4571	14.0103	12.6404	11.5406	11.0231
		FSBT [10]	17.8711	15.4250	14.0030	12.7120	11.8157	11.3073
		TSBT [21]	17.8812	15.4588	14.0100	12.6405	11.5431	11.0240
	3	Present	34.2143	29.8367	27.1014	24.3168	21.7112	20.5561
		FSBT [10]	34.1449	29.7146	27.0525	24.4970	22.4642	21.3219
		TSBT [21]	34.2097	29.8382	27.0979	24.3152	21.7158	20.5561
20	1	Present	5.4603	4.6506	4.2051	3.8361	3.6485	3.5390
		FSBT [10]	5.4603	4.6504	4.2051	3.8368	3.6509	3.5416
		TSBT [21]	5.4603	4.6511	4.2051	3.8361	3.6485	3.5390
	2	Present	21.5732	18.3942	16.6344	15.1618	14.3742	13.9261
		FSBT [10]	21.5732	18.3912	16.6344	15.1715	14.4110	13.9653
		TSBT [21]	21.5732	18.3962	16.6344	15.1619	14.3746	13.9263
	3	Present	47.5999	40.6543	36.7736	33.4735	31.5804	30.5400
		FSBT [10]	47.5921	40.6335	36.7673	33.5135	31.7473	30.7176
		TSBT [21]	47.5930	40.6526	36.7679	33.4689	31.5780	30.5369

Table 4: Comparison of the nondimensional fundamental natural frequency of FG beams with various boundary conditions (L/h=5 and 20, type A).

L/h	BC	Theory	p					
			0	0.5	1	2	5	10
5	S-S	Present	5.1528	4.4102	3.9904	3.6264	3.4009	3.2815
		FSBT [10]	5.1525	4.4075	3.9902	3.6344	3.4312	3.3135
		TSBT [21]	5.1527	4.4107	3.9904	3.6264	3.4012	3.2816
	C-C	Present	10.0726	8.7463	7.9518	7.1776	6.4929	6.1658
		FSBT [22]	10.0705	8.7467	7.9503	7.1767	6.4935	6.1652
		TSBT [22]	10.0699	8.7463	7.9499	7.1766	6.4940	6.1652
	C-F	Present	1.8957	1.6182	1.4636	1.3328	1.2594	1.2187
		FSBT [22]	1.8948	1.6174	1.4630	1.3338	1.2645	1.2240
		TSBT [22]	1.8952	1.6182	1.4633	1.3325	1.2592	1.2183
20	S-S	Present	5.4603	4.6506	4.2051	3.8361	3.6485	3.5390
		FSBT [22]	5.4603	4.6514	4.2051	3.8368	3.6509	3.5416
		TSBT [22]	5.4603	4.6516	4.2050	3.8361	3.6485	3.5390
		TSBT [21]	5.4603	4.6511	4.2051	3.8361	3.6485	3.5390
	C-C	Present	12.2243	10.4269	9.4319	8.5977	8.1446	7.8860
		FSBT [22]	12.2235	10.4263	9.4314	8.6040	8.1699	7.9128
		TSBT [22]	12.2238	10.4287	9.4316	8.5975	8.1448	7.8859
	C-F	Present	1.9496	1.6602	1.5011	1.3696	1.3034	1.2646
		FSBT [22]	1.9496	1.6604	1.5010	1.3697	1.3038	1.2650
		TSBT [22]	1.9495	1.6605	1.5011	1.3696	1.3033	1.2645

Table 5: Comparison of the nondimensional critical buckling load of FG beams with various boundary conditions (L/h=5 and 10, type A).

L/h	BC	Theory	p					
			0	0.5	1	2	5	10
5	S-S	Present	48.8406	32.0013	24.6894	19.1577	15.7355	14.1448
		FSBT [10]	48.8350	31.9980	24.6810	19.1230	15.6970	14.1300
		FSBT [9]	48.8350	31.9670	24.6870	19.2450	16.0240	14.4270
		TSBT [17]	48.8401	32.0094	24.6911	19.1605	15.7400	14.1468
	C-C	Present	154.5610	103.7167	80.5940	61.7666	47.7174	41.7885
		FSBT [9]	154.3500	103.2200	80.4980	62.6140	50.3840	44.2670
		TSBT [17]	154.5500	103.7490	80.6087	61.7925	47.7562	41.8042
	C-F	Present	13.0771	8.5000	6.5427	5.0977	4.2772	3.8820
		FSBT [9]	13.2130	8.5782	6.6002	5.1495	4.3445	3.9501
		TSBT [17]	13.0771	8.5020	6.5428	5.0979	4.2776	3.8821
10	S-S	Present	52.3083	34.0002	26.1707	20.3909	17.1091	15.5278
		FSBT [10]	52.3080	34.0000	26.1690	20.3820	17.0980	15.5240
		FSBT [9]	52.3090	33.9960	26.1710	20.4160	17.1920	15.6120
		TSBT [17]	52.3082	34.0087	26.1727	20.3936	17.1118	15.5291
	C-C	Present	195.3623	128.0053	98.7885	76.6538	62.9580	56.5926
		FSBT [9]	195.3400	127.8700	98.7490	76.9800	64.0960	57.7080
		TSBT [17]	195.3610	128.0500	98.7868	76.6677	62.9786	56.5971
	C-F	Present	13.3741	8.6694	6.6678	5.2025	4.3974	4.0045
		FSBT [9]	13.2130	8.5666	6.6570	5.1944	4.3903	3.9969
		TSBT [17]	13.3742	8.6714	6.6680	5.2027	4.3976	4.0046

Table 6: The first five natural frequencies of a cantilever sandwich beam with a FG core and isotropic faces (p=1).

Mode	Bui et al. [42]		Mashat et al. [26]		Present
	ANSYS	Meshfree	TE1^{zz}	E4-4$_2$	
1	459.50	459.40	459.10	461.90	459.20
2	2708.70	2708.70	2710.50	2724.30	2713.50
3	6440.80	6440.70	6433.60	6455.10	6433.70
4	6991.40	6995.80	7005.10	7035.90	7031.20
5	12446.00	12446.40	12484.20	12531.70	12534.70

Table 7: Nondimensional fundamental frequency ($\bar{\omega}$) of FG sandwich beams with various boundary conditions (L/h=5, type B).

BC	p	Theory	1-0-1	2-1-2	2-1-1	1-1-1	2-2-1	1-2-1
S-S	0	Present	5.1528	5.1528	5.1528	5.1528	5.1528	5.1528
		TSBT [17]	5.1528	5.1528	5.1528	5.1528	5.1528	5.1528
	0.5	Present	4.1254	4.2340	4.2943	4.3294	4.4045	4.4791
		TSBT [17]	4.1268	4.2351	4.2945	4.3303	4.4051	4.4798
	1	Present	3.5736	3.7298	3.8206	3.8756	3.9911	4.1105
		TSBT [17]	3.5735	3.7298	3.8187	3.8755	3.9896	4.1105
	2	Present	3.0682	3.2366	3.3546	3.4190	3.5719	3.7334
		TSBT [17]	3.0680	3.2365	3.3514	3.4190	3.5692	3.7334
	5	Present	2.7450	2.8441	2.9790	3.0182	3.1966	3.3771
		TSBT [17]	2.7446	2.8439	2.9746	3.0181	3.1928	3.3771
	10	Present	2.6936	2.7357	2.8716	2.8810	3.0630	3.2357
		TSBT [17]	2.6932	2.7355	2.8669	2.8808	3.0588	3.2356
C-C	0	Present	10.0726	10.0726	10.0726	10.0726	10.0726	10.0726
		TSBT [17]	10.0678	10.0678	10.0678	10.0678	10.0678	10.0678
	0.5	Present	8.3606	8.5736	8.6688	8.7442	8.8654	8.9969
		TSBT [17]	8.3600	8.5720	8.6673	8.7423	8.8648	8.9942
	1	Present	7.3707	7.6910	7.8428	7.9623	8.1593	8.3747
		TSBT [17]	7.3661	7.6865	7.8390	7.9580	8.1554	8.3705
	2	Present	6.4139	6.7867	6.9939	7.1412	7.4138	7.7149
		TSBT [17]	6.4095	6.7826	6.9908	7.1373	7.4105	7.7114
	5	Present	5.7315	6.0335	6.2765	6.3925	6.7216	7.0723
		TSBT [17]	5.7264	6.0293	6.2737	6.3889	6.7188	7.0691
	10	Present	5.5429	5.8104	6.0555	6.1278	6.4668	6.8119
		TSBT [17]	5.5375	5.8059	6.0527	6.1240	6.4641	6.8087
C-F	0	Present	1.8953	1.8953	1.8953	1.8953	1.8953	1.8953
		TSBT [17]	1.8952	1.8952	1.8952	1.8952	1.8952	1.8952
	0.5	Present	1.5064	1.5463	1.5693	1.5819	1.6104	1.6383
		TSBT [17]	1.5069	1.5466	1.5696	1.5821	1.6108	1.6384
	1	Present	1.3008	1.3576	1.3919	1.4115	1.4550	1.4993
		TSBT [17]	1.3007	1.3575	1.3918	1.4115	1.4549	1.4992
	2	Present	1.1143	1.1747	1.2189	1.2416	1.2987	1.3582
		TSBT [17]	1.1143	1.1746	1.2188	1.2416	1.2986	1.3582
	5	Present	0.9974	1.0304	1.0807	1.0936	1.1598	1.2258
		TSBT [17]	0.9973	1.0303	1.0806	1.0935	1.1597	1.2257
	10	Present	0.9813	0.9910	1.0417	1.0432	1.1106	1.1734
		TSBT [17]	0.9812	0.9909	1.0416	1.0431	1.1106	1.1734

Table 8: Nondimensional fundamental frequency ($\bar{\omega}$) of FG sandwich beams with various boundary conditions (L/h=20, type B).

BC	p	Theory	1-0-1	2-1-2	2-1-1	1-1-1	2-2-1	1-2-1
S-S	0	Present	5.4603	5.4603	5.4603	5.4603	5.4603	5.4603
		TSBT [17]	5.4603	5.4603	5.4603	5.4603	5.4603	5.4603
	0.5	Present	4.3132	4.4278	4.4960	4.5315	4.6158	4.6972
		TSBT [17]	4.3148	4.4290	4.4970	4.5324	4.6170	4.6979
	1	Present	3.7147	3.8768	3.9775	4.0328	4.1603	4.2889
		TSBT [17]	3.7147	3.8768	3.9774	4.0328	4.1602	4.2889
	2	Present	3.1764	3.3465	3.4756	3.5389	3.7051	3.8769
		TSBT [17]	3.1764	3.3465	3.4754	3.5389	3.7049	3.8769
	5	Present	2.8440	2.9311	3.0776	3.1111	3.3030	3.4921
		TSBT [17]	2.8439	2.9310	3.0773	3.1111	3.3028	3.4921
	10	Present	2.8042	2.8188	2.9665	2.9662	3.1616	3.3406
		TSBT [17]	2.8041	2.8188	2.9662	2.9662	3.1613	3.3406
C-C	0	Present	12.2243	12.2243	12.2243	12.2243	12.2243	12.2243
		TSBT [17]	12.2228	12.2228	12.2228	12.2228	12.2228	12.2228
	0.5	Present	9.6916	9.9484	10.0985	10.1788	10.3647	10.5455
		TSBT [17]	9.6942	9.9501	10.1001	10.1800	10.3668	10.5460
	1	Present	8.3601	8.7248	8.9479	9.0729	9.3555	9.6419
		TSBT [17]	8.3594	8.7241	8.9474	9.0722	9.3550	9.6411
	2	Present	7.1568	7.5422	7.8293	7.9732	8.3431	8.7268
		TSBT [17]	7.1563	7.5417	7.8293	7.9727	8.3430	8.7262
	5	Present	6.4071	6.6121	6.9387	7.0174	7.4459	7.8696
		TSBT [17]	6.4064	6.6116	6.9389	7.0170	7.4461	7.8692
	10	Present	6.3094	6.3595	6.6887	6.6928	7.1293	7.5315
		TSBT [17]	6.3086	6.3590	6.6889	6.6924	7.1296	7.5311
C-F	0	Present	1.9496	1.9496	1.9496	1.9496	1.9496	1.9496
		TSBT [17]	1.9496	1.9496	1.9496	1.9496	1.9496	1.9496
	0.5	Present	1.5392	1.5801	1.6045	1.6171	1.6473	1.6764
		TSBT [17]	1.5397	1.5805	1.6048	1.6175	1.6477	1.6766
	1	Present	1.3253	1.3831	1.4191	1.4388	1.4844	1.5304
		TSBT [17]	1.3253	1.3831	1.4191	1.4388	1.4844	1.5304
	2	Present	1.1330	1.1937	1.2398	1.2623	1.3217	1.3831
		TSBT [17]	1.1330	1.1937	1.2398	1.2623	1.3217	1.3831
	5	Present	1.0145	1.0454	1.0977	1.1096	1.1781	1.2456
		TSBT [17]	1.0145	1.0453	1.0977	1.1096	1.1781	1.2456
	10	Present	1.0005	1.0053	1.0581	1.0578	1.1276	1.1915
		TSBT [17]	1.0005	1.0053	1.0581	1.0578	1.1276	1.1915

Table 9: Nondimensional critical buckling load ($\bar{N}_{cr}$) of FG sandwich beams with various boundary conditions (L/h=5, type B).

BC	p	Theory	1-0-1	2-1-2	2-1-1	1-1-1	2-2-1	1-2-1
S-S	0	Present	48.5964	48.5964	48.5964	48.5964	48.5964	48.5964
		TSBT [17]	48.5959	48.5959	48.5959	48.5959	48.5959	48.5959
	0.5	Present	27.8380	30.0146	31.0577	31.8650	33.2336	34.7546
		TSBT [17]	27.8574	30.0301	31.0728	31.8784	33.2536	34.7653
	1	Present	19.6541	22.2121	23.5250	24.5602	26.3611	28.4440
		TSBT [17]	19.6525	22.2108	23.5246	24.5596	26.3611	28.4447
	2	Present	13.5820	15.9167	17.3254	18.3596	20.3751	22.7859
		TSBT [17]	13.5801	15.9152	17.3249	18.3587	20.3750	22.7863
	5	Present	10.1488	11.6697	13.0279	13.7226	15.7313	18.0915
		TSBT [17]	10.1460	11.6676	13.0270	13.7212	15.7307	18.0914
	10	Present	9.4543	10.5370	11.8380	12.2621	14.2002	16.3789
		TSBT [17]	9.4515	10.5348	11.8370	12.2605	14.1995	16.3783
C-C	0	Present	152.1588	152.1588	152.1588	152.1588	152.1588	152.1588
		TSBT [17]	152.1470	152.1470	152.1470	152.1470	152.1470	152.1470
	0.5	Present	92.8202	99.9361	102.8605	105.6331	109.5284	114.1312
		TSBT [17]	92.8833	99.9860	102.9120	105.6790	109.6030	114.1710
	1	Present	67.5184	76.2801	80.1730	83.8267	89.2223	95.7230
		TSBT [17]	67.4983	76.2634	80.1670	83.8177	89.2208	95.7287
	2	Present	47.7247	56.2259	60.6127	64.4352	70.7590	78.5570
		TSBT [17]	47.7010	56.2057	60.6056	64.4229	70.7563	78.5608
	5	Present	35.5811	42.0298	46.3852	49.2949	55.8338	63.7847
		TSBT [17]	35.5493	42.0033	46.3743	49.2763	55.8271	63.7824
	10	Present	32.3345	38.0239	42.2062	44.3593	50.7406	58.2532
		TSBT [17]	32.3019	37.9944	42.1935	44.3374	50.7315	58.2461
C-F	0	Present	13.0595	13.0595	13.0595	13.0595	13.0595	13.0595
		TSBT [17]	13.0594	13.0594	13.0594	13.0594	13.0594	13.0594
	0.5	Present	7.3263	7.9026	8.1912	8.4016	8.7789	9.1913
		TSBT [17]	7.3314	7.9068	8.1951	8.4051	8.7839	9.1940
	1	Present	5.1246	5.7922	6.1490	6.4166	6.9050	7.4638
		TSBT [17]	5.1245	5.7921	6.1490	6.4166	6.9050	7.4639
	2	Present	3.5175	4.1157	4.4927	4.7564	5.2952	5.9347
		TSBT [17]	3.5173	4.1156	4.4927	4.7564	5.2952	5.9348
	5	Present	2.6301	3.0006	3.3609	3.5311	4.0621	4.6806
		TSBT [17]	2.6298	3.0004	3.3609	3.5310	4.0620	4.6806
	10	Present	2.4685	2.7078	3.0528	3.1489	3.6596	4.2268
		TSBT [17]	2.4683	2.7077	3.0527	3.1488	3.6595	4.2267

Table 10: Nondimensional critical buckling load ($\bar{N}_{cr}$) of FG sandwich beams with various boundary conditions (L/h=20, type B).

BC	p	Theory	1-0-1	2-1-2	2-1-1	1-1-1	2-2-1	1-2-1
S-S	0	Present	53.2364	53.2364	53.2364	53.2364	53.2364	53.2364
		TSBT [17]	53.2364	53.2364	53.2364	53.2364	53.2364	53.2364
	0.5	Present	29.6965	32.0368	33.2217	34.0722	35.6202	37.3054
		TSBT [17]	29.7175	32.2629	33.2376	34.0862	35.6405	37.3159
	1	Present	20.7213	23.4212	24.8793	25.9588	27.9537	30.2306
		TSBT [17]	20.7212	23.4211	24.8796	25.9588	27.9540	30.2307
	2	Present	14.1974	16.6051	18.1400	19.2000	21.3923	23.9899
		TSBT [17]	14.1973	16.6050	18.1404	19.3116	21.3927	23.9900
	5	Present	10.6176	12.0886	13.5520	14.2285	16.3829	18.8874
		TSBT [17]	10.6171	12.0883	13.5523	14.2284	16.3834	18.8874
	10	Present	9.9850	10.9075	12.3081	12.6820	14.7520	17.0445
		TSBT [17]	9.9847	10.9075	12.3084	12.6819	14.7525	17.0443
C-C	0	Present	208.9515	208.9515	208.9515	208.9515	208.9515	208.9515
		TSBT [17]	208.9510	208.9510	208.9510	208.9510	208.9510	208.9510
	0.5	Present	117.2200	126.4422	131.0594	134.4255	140.4622	147.0614
		TSBT [17]	117.3030	126.5080	131.1240	134.4810	140.5450	147.1040
	1	Present	81.9944	92.6754	98.3839	102.6655	110.4792	119.4215
		TSBT [17]	81.9927	92.6741	98.3880	102.6650	110.4830	119.4220
	2	Present	56.2793	65.8505	71.8837	76.1030	84.7230	94.9558
		TSBT [17]	56.2773	65.8489	71.8900	76.1020	84.7291	94.9563
	5	Present	42.0814	48.0095	53.7751	56.4973	64.9930	74.8903
		TSBT [17]	42.0775	48.0070	53.7820	56.4958	65.0007	74.8903
	10	Present	39.4962	43.3252	48.8443	50.3827	58.5529	67.6281
		TSBT [17]	39.4930	43.3233	48.8510	50.3811	58.5607	67.6270
C-F	0	Present	13.3730	13.3730	13.3730	13.3730	13.3730	13.3730
		TSBT [17]	13.3730	13.3730	13.3730	13.3730	13.3730	13.3730
	0.5	Present	7.4490	8.0363	8.3345	8.5477	8.9372	9.3607
		TSBT [17]	7.4543	8.0405	8.3385	8.5512	8.9422	9.3634
	1	Present	5.1944	5.8713	6.2378	6.5083	7.0096	7.5815
		TSBT [17]	5.1944	5.8713	6.2378	6.5083	7.0096	7.5815
	2	Present	3.5574	4.1603	4.5457	4.8110	5.3615	6.0134
		TSBT [17]	3.5574	4.1603	4.5457	4.8110	5.3615	6.0134
	5	Present	2.6606	3.0276	3.3948	3.5637	4.1042	4.7323
		TSBT [17]	2.6605	3.0275	3.3948	3.5637	4.1043	4.7323
	10	Present	2.5033	2.7317	3.0831	3.1759	3.6952	4.2698
		TSBT [17]	2.5032	2.7317	3.0832	3.1759	3.6952	4.2698

Table 11: The first three nondimensional natural frequencies of FG sandwich beams with various boundary conditions (type C).

Mode	Scheme	L/h	BC	p					
				0	0.5	1	2	5	10
1	1-2-1	5	S-S	4.0691	3.7976	3.6636	3.5530	3.4914	3.4830
			C-C	8.3282	7.7553	7.4487	7.1485	6.8702	6.7543
			C-F	1.4840	1.3865	1.3393	1.3022	1.2857	1.2867
		20	S-S	4.2445	3.9695	3.8387	3.7402	3.7081	3.7214
			C-C	9.5451	8.9243	8.6264	8.3959	8.3047	8.3205
			C-F	1.5145	1.4165	1.3700	1.3350	1.3241	1.3292
	2-2-1	5	S-S	3.6624	3.5692	3.5292	3.5002	3.4858	3.4830
			C-C	7.5709	7.2636	7.0901	6.9040	6.8998	6.5941
			C-F	1.3344	1.3050	1.2939	1.2884	1.2903	1.2930
		20	S-S	3.8136	3.7406	3.7177	3.7144	3.7380	3.7552
			C-C	8.5832	8.4064	8.3442	8.3205	8.3488	8.3738
			C-F	1.3607	1.3350	1.3271	1.3263	1.3353	1.3418
2	1-2-1	5	S-S	14.5921	13.5629	13.0215	12.5117	12.0822	11.9168
			C-C	19.8886	18.4463	17.6290	16.7552	15.8266	15.3878
			C-F	8.3149	7.7255	7.4173	7.1308	6.8984	6.8139
		20	S-S	16.8284	15.7307	15.2043	14.7986	14.6424	14.6748
			C-C	25.9323	24.2300	23.4015	22.7371	22.4123	22.4014
			C-F	9.4133	8.8002	8.5069	8.2819	8.1986	8.2195
	2-2-1	5	S-S	13.1913	12.6833	12.4117	12.1315	11.8448	11.7177
			C-C	18.1865	17.1905	16.5950	15.9164	15.1574	14.8131
			C-F	7.5021	7.2215	7.0739	6.9254	6.7792	6.7161
		20	S-S	15.1255	14.8149	14.7073	14.6700	14.7283	14.7777
			C-C	23.3403	22.8045	22.5913	22.4619	22.4443	22.4623
			C-F	8.4598	8.2890	8.2312	8.2137	8.2512	8.2814
3	1-2-1	5	S-S	28.7653	26.6542	25.4901	24.3022	23.1254	22.5934
			C-C	34.0624	31.5260	30.0458	28.4068	26.5927	25.7241
			C-F	14.0712	13.2130	12.7196	12.1683	11.5477	11.2377
		20	S-S	37.3334	34.8731	33.6782	32.7268	32.2818	32.2861
			C-C	49.8846	46.5716	44.9326	43.5667	42.7705	42.6332
			C-F	26.0193	24.3084	23.4799	22.8254	22.5324	22.5472
	2-2-1	5	S-S	26.4473	24.8325	24.0825	23.2485	22.3275	21.9082
			C-C	31.2772	29.2997	28.1131	26.7610	25.2645	24.5968
			C-F	13.3087	12.5064	12.0503	11.5480	10.9899	10.7150
		20	S-S	33.5757	32.8132	32.5173	32.3519	32.3630	32.4104
			C-C	44.9445	43.7848	43.2741	42.8808	42.6431	42.5723
			C-F	23.3958	22.8769	22.6806	22.5797	22.6081	22.6521

Table 12: Nondimensional critical buckling load of FG sandwich beams with various boundary conditions (type C).

Scheme	L/h	BC	p					
			0	0.5	1	2	5	10
1-2-1	5	S-S	27.9314	22.9869	20.7762	18.9588	17.7320	17.3775
		C-C	94.6117	77.5129	69.4877	62.2249	55.9446	53.3734
		C-F	7.3149	6.0286	5.4629	5.0154	4.7534	4.7024
	20	S-S	29.6120	24.4140	22.1386	20.3581	19.3639	19.2058
		C-C	117.0384	96.4573	87.4069	80.2465	76.0539	75.2379
		C-F	7.4254	6.1225	5.5529	5.1084	4.8634	4.8269
2-2-1	5	S-S	21.5207	19.4909	18.5897	17.8178	17.1942	16.9422
		C-C	74.0960	65.2766	60.8501	56.4008	51.9303	49.9605
		C-F	5.6078	5.1228	4.9221	4.7709	4.6809	4.6533
	20	S-S	22.6714	20.7578	19.9839	19.4292	19.1504	19.0848
		C-C	89.7255	81.9647	78.7529	76.3344	74.8949	74.4533
		C-F	5.6831	5.2064	5.0148	4.8794	4.8150	4.8016

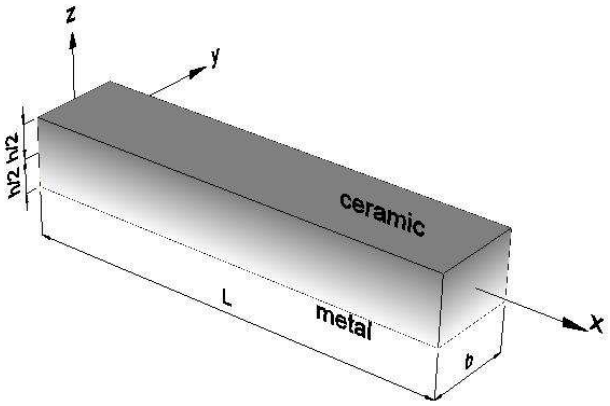

(a) FG beams with length L and section $b \times h$

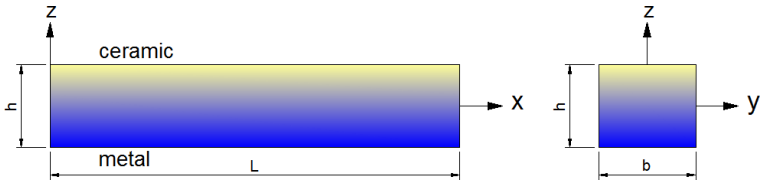

(b) Type A

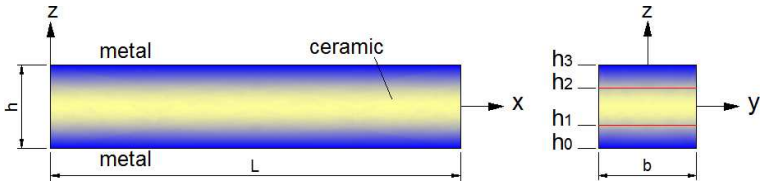

(c) Type B

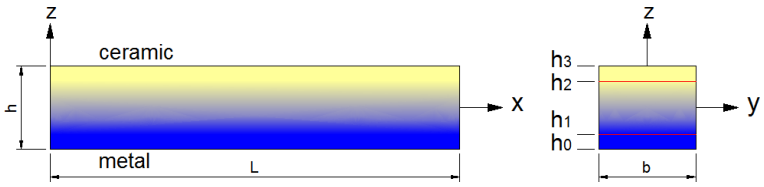

(d) Type C

Figure 1: Geometry of isotropic and FG sandwich beams.

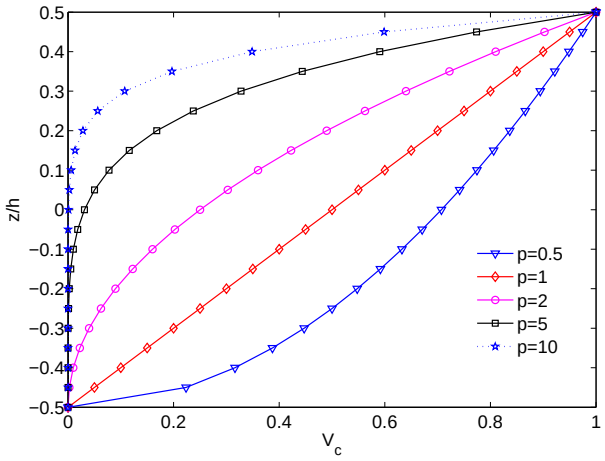

(a) Type A

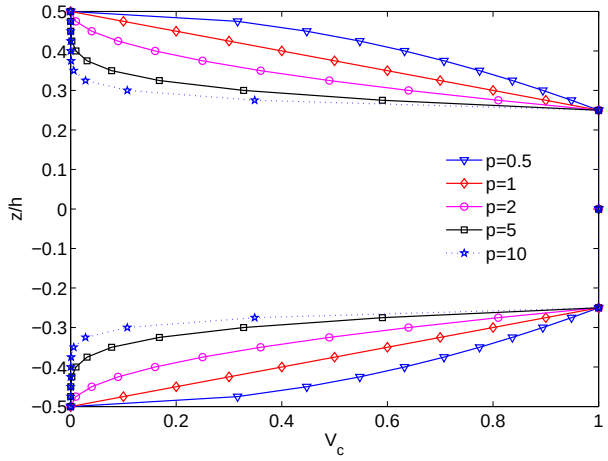

(b) Type B (1-2-1)

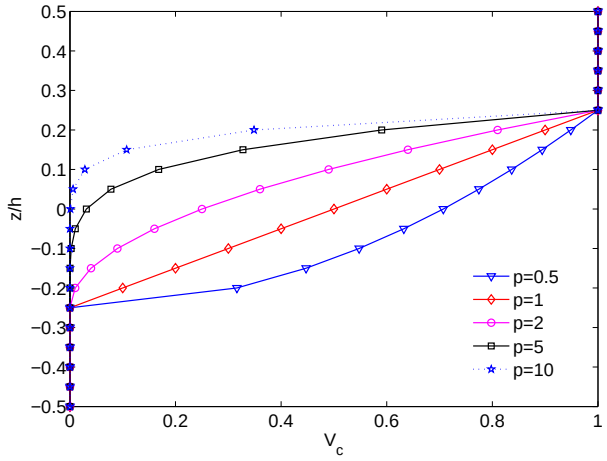

(c) Type C (1-2-1)

Figure 2: Distribution of ceramic material through the beam depth according to the power-law form.

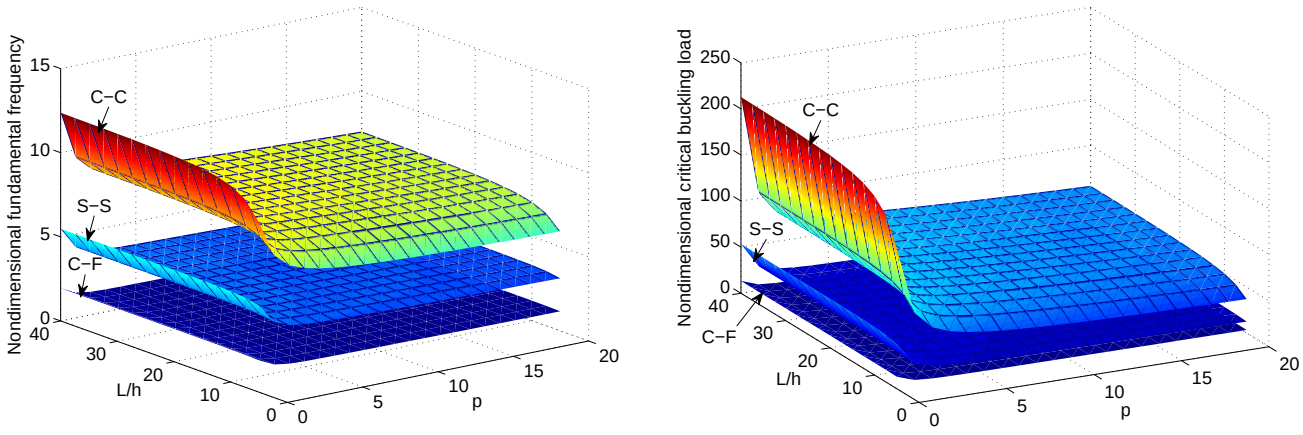

(a) (b)

Figure 3: Effects of the power-law index p and span-to-depth ratio L/h on the nondimensional fundamental frequency ($\bar{\omega}$) and critical buckling load ($\bar{N}_{cr}$) of FG beams (type A).

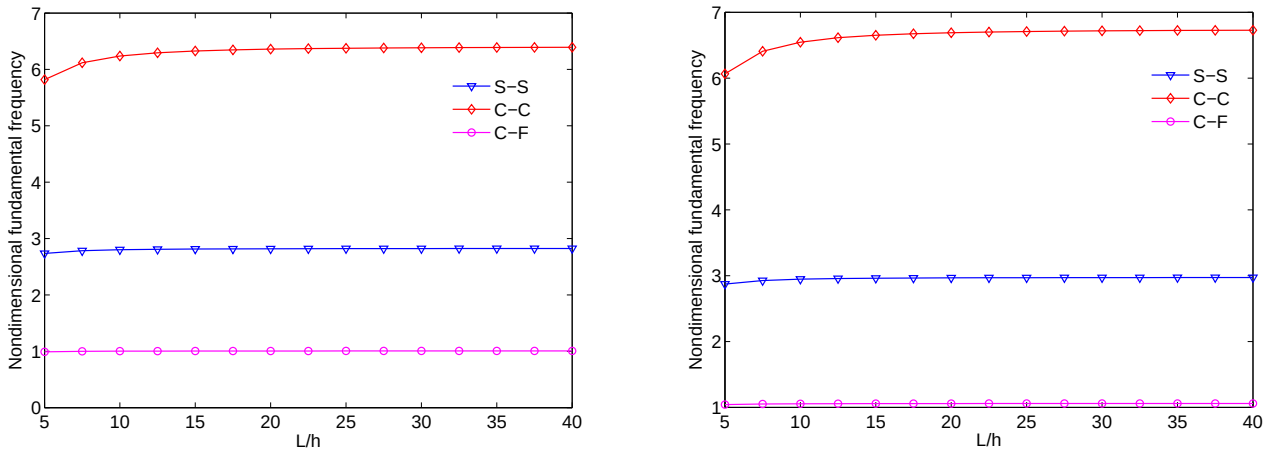

(a) 2-1-2

(b) 2-1-1

Figure 4: Variation of the nondimensional fundamental frequency of FG sandwich beams ($p = 10$) with respect to the span-to-depth ratio L/h (type B).

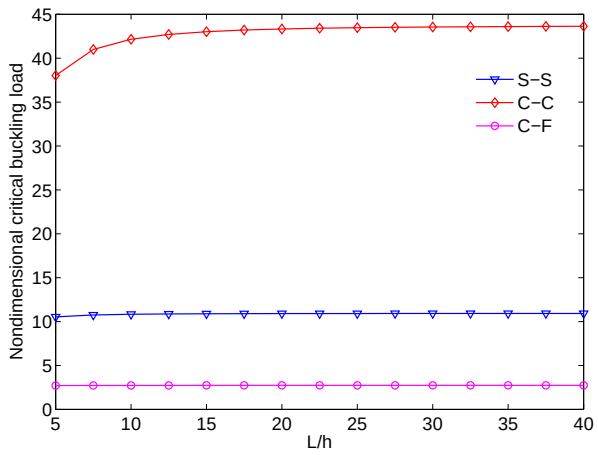

(a) 2-1-2

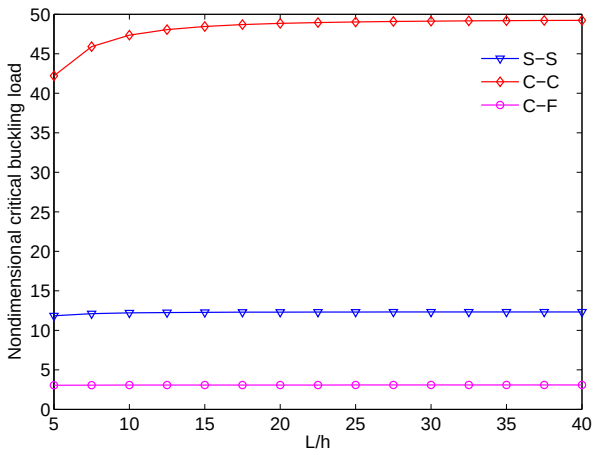

(b) 2-1-1

Figure 5: Variation of the nondimensional critical buckling load of FG sandwich beams ($p = 10$) with respect to the span-to-depth ratio L/h (type B).

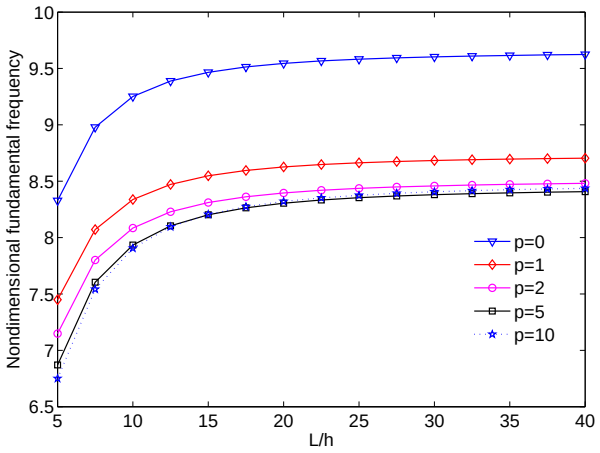

(a) 1-2-1

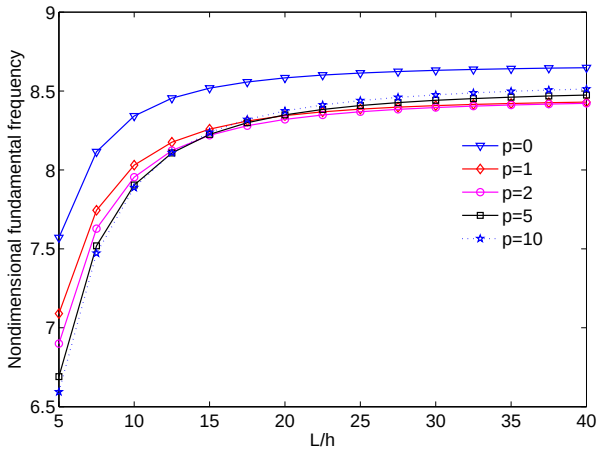

(b) 2-2-1

Figure 6: Variation of the nondimensional fundamental frequency of (C-C) FG sandwich beams with respect to the span-to-depth ratio L/h (type C).

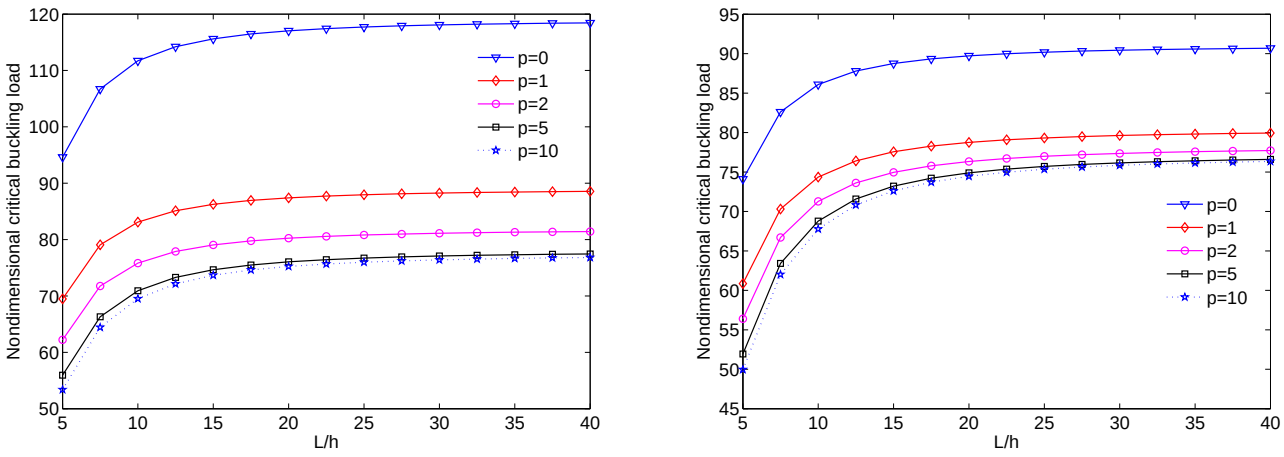

(a) 1-2-1

(b) 2-2-1

Figure 7: Variation of the nondimensional critical buckling load of (C-C) FG sandwich beams with respect to the span-to-depth ratio L/h (type C).

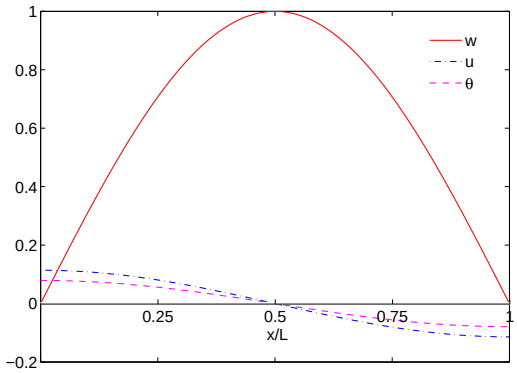

(a) Mode 1, $\bar{\omega}_1$=3.4830 (1-2-1)

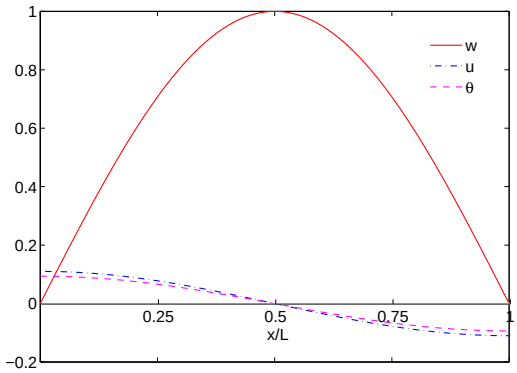

(b) Mode 1, $\bar{\omega}_1$=3.4830 (2-2-1)

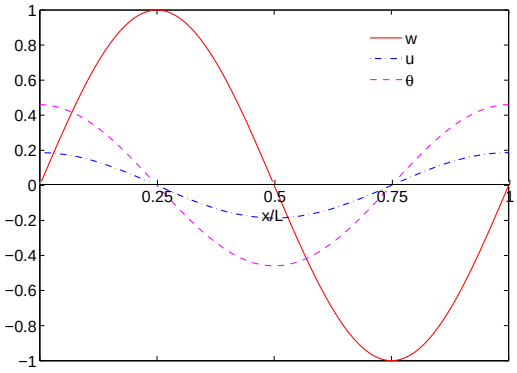

(c) Mode 2, $\bar{\omega}_2$=11.9168 (1-2-1)

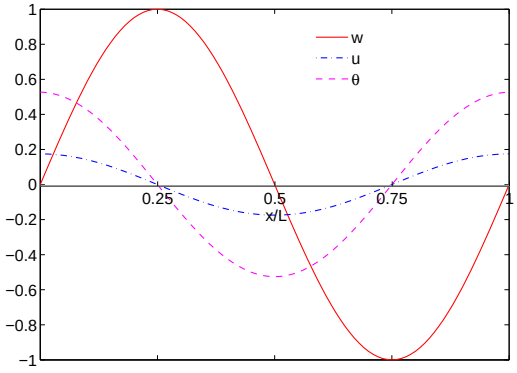

(d) Mode 2, $\bar{\omega}_2$=11.7177 (2-2-1)

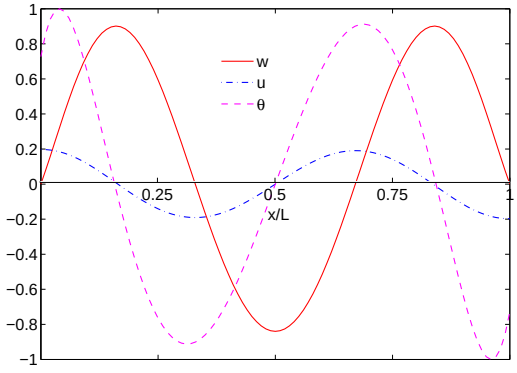

(e) Mode 3, $\bar{\omega}_3$=22.5934 (1-2-1)

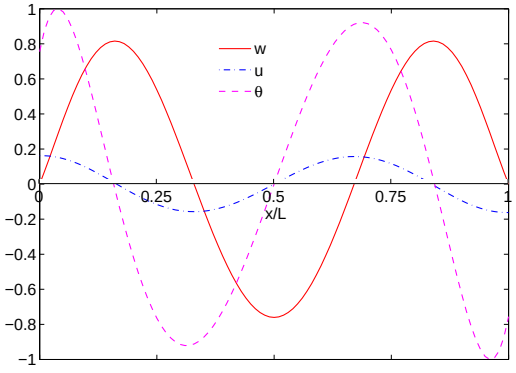

(f) Mode 3, $\bar{\omega}_3$=21.9082 (2-2-1)

Figure 8: The first three mode shapes of (1-2-1) and (2-2-1) (S-S) FG sandwich beams ($L/h = 5$, $p = 10$, type C).